Science and Technology Facilities Council

Measurement of $e^+e^- \rightarrow \pi^+\pi^-\pi^0$ with ISR events at BaBar and its contribution to $(g\text{-}2)_\mu$

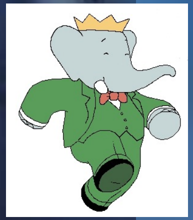

Fergus Wilson

Rutherford Appleton Laboratory

On behalf of the BaBar Collaboration

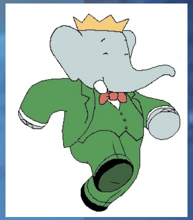

g-2 Theory Workshop, 5th – 9th September, Edinburgh, 2022

Outline

- Recent BaBar results with three pions:
  - Measurement of $e^+e^- \to \pi^+\pi^-\pi^0$ cross-section
    - [Phys Rev D 104, 112003 (2021)] $\leftarrow$ Main result
- Contribution to $(g\text{-}2)_\mu$ from $e^+e^- \to \pi^+\pi^-\pi^0$
- Recent BaBar results with multiple pions and kaons:
  - Measurements of $e^+e^- \to \pi^+\pi^-4\pi^0$ cross-section
    - Phys Rev D 104, 112004 (2021)
  - Measurements of $e^+e^- \to 2(\pi^+\pi^-)3\pi^0$ cross-section
    - Phys Rev D 103, 092001 (2021)
  - Preliminary measurements of $e^+e^- \to KK\pi\pi\pi$ cross-sections
    - arXiv:2207.10340 (2022)
- Conclusion

$e^+e^- \longrightarrow \pi^+\pi^-\pi^0$ contribution to $a_\mu = (g\text{-}2)_\mu/2$

- SM prediction: $$a_\mu^{SM} = \frac{(g-2)_\mu}{2} = a_\mu^{QED} + a_\mu^{EW} + a_\mu^{Had}$$
- Leading order hadronic contribution:

$$a_\mu^{Had,LO} = \frac{\alpha^2}{3\pi^2} \int_{m_\pi^2}^{\infty} \frac{K(s)}{s} \frac{\sigma_0(e^+e^- \to hadrons)(s)}{4\pi\alpha^2/3s}$$

$$K(s) = \frac{x^2}{2}(2-x^2) + \frac{(1+x^2)(1+x)^2}{x^2}\left(\log(1+x) - x + \frac{x^2}{2}\right) + \frac{1+x}{1-x}x^2 \log x$$

$$x = \frac{1-\beta}{1+\beta},\ \beta = \sqrt{1-4m_\mu^2/s}$$

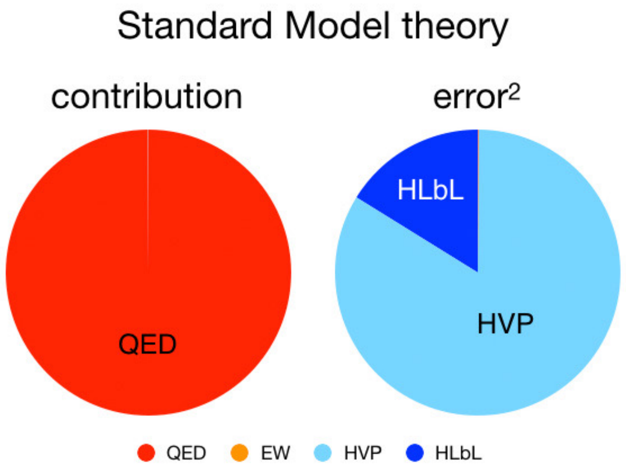

$a_\mu^{had,LO\text{-}VP}$ $\quad$ $a_\mu^{had,LO\text{-}VP}$ error squared

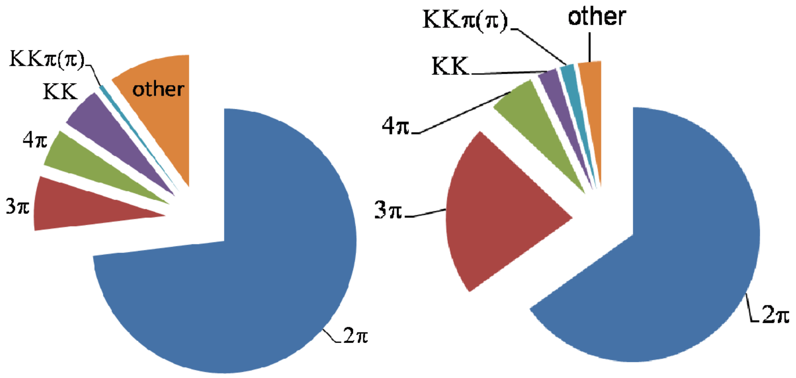

- (for details, see [1] for example)
- $e^+e^- \to \pi^+\pi^-$ contributes ~73% to $a_\mu^{Had,LO}$
- $e^+e^- \to \pi^+\pi^-\pi^0$ *contributes* ~7% to $a_\mu^{Had,LO}$ and ~19% to the uncertainty [2]

Existing cross-sections

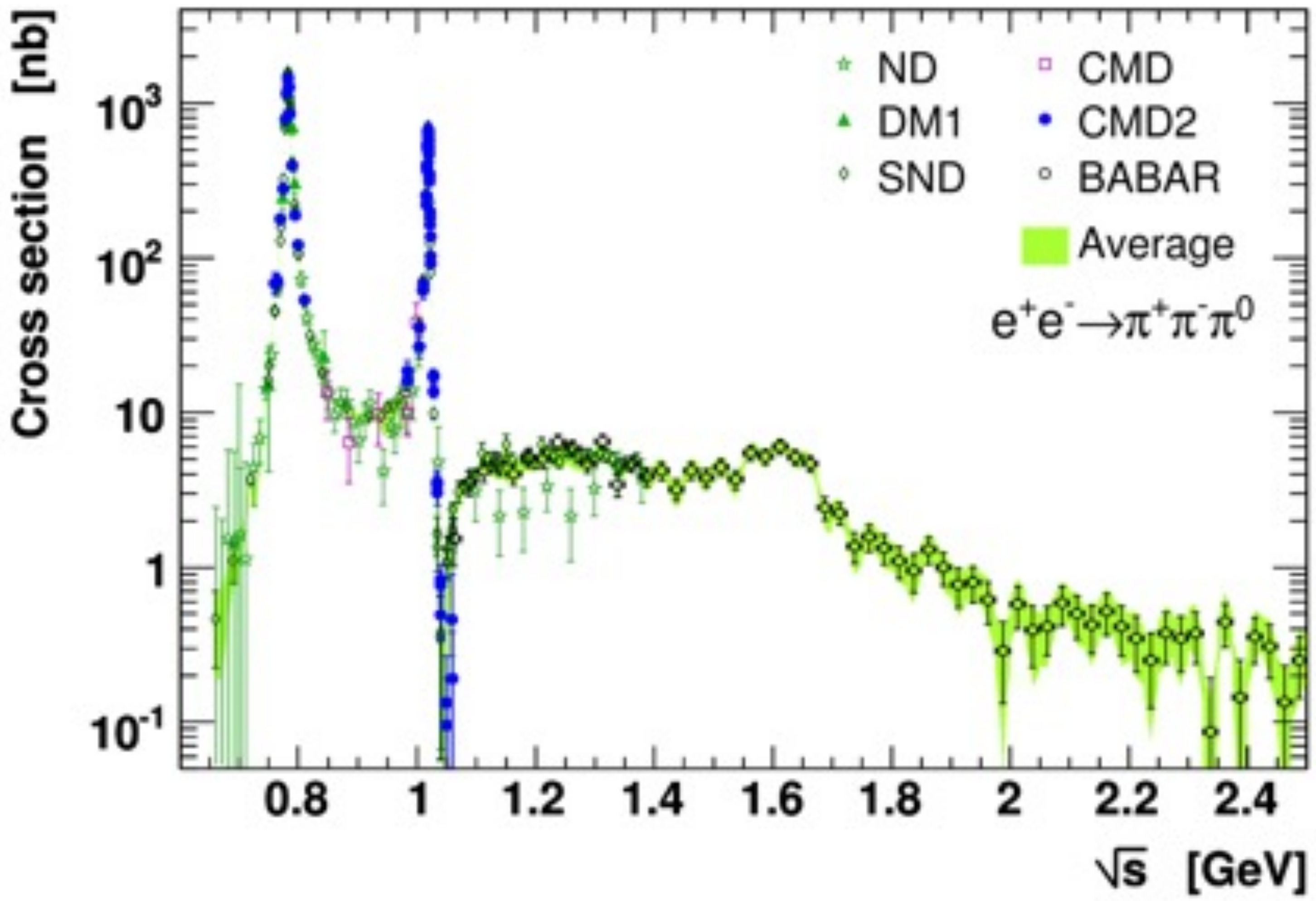

Previous BaBar $\pi^+\pi^-\pi^0$ [8]

- No result below 1.05 GeV
- Only used 89.3 fb^{-1}

Experimental differences contribute to uncertainty e.g. 8% difference between SND and CMD2 near ω

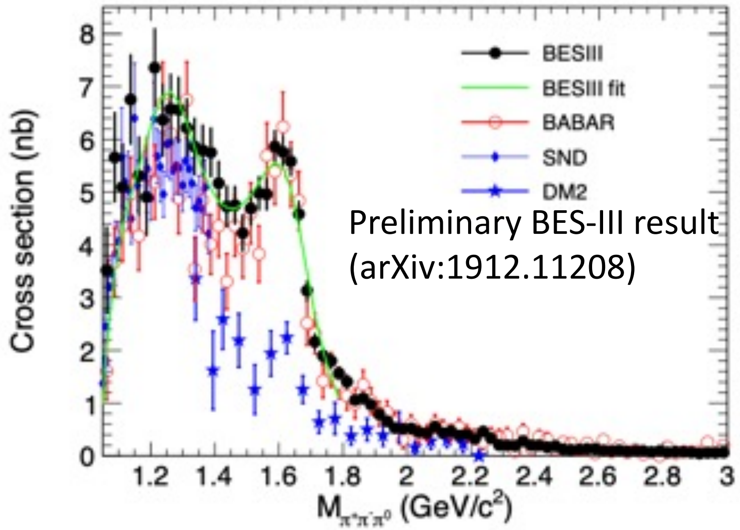

Preliminary BES-III result (arXiv:1912.11208)

BaBar at SLAC PEP-II: 1999 - 2008

- Asymmetric beam energies nominally colliding 3.1 GeV e^+ and 9.0 GeV e^- at Υ(nS) resonances

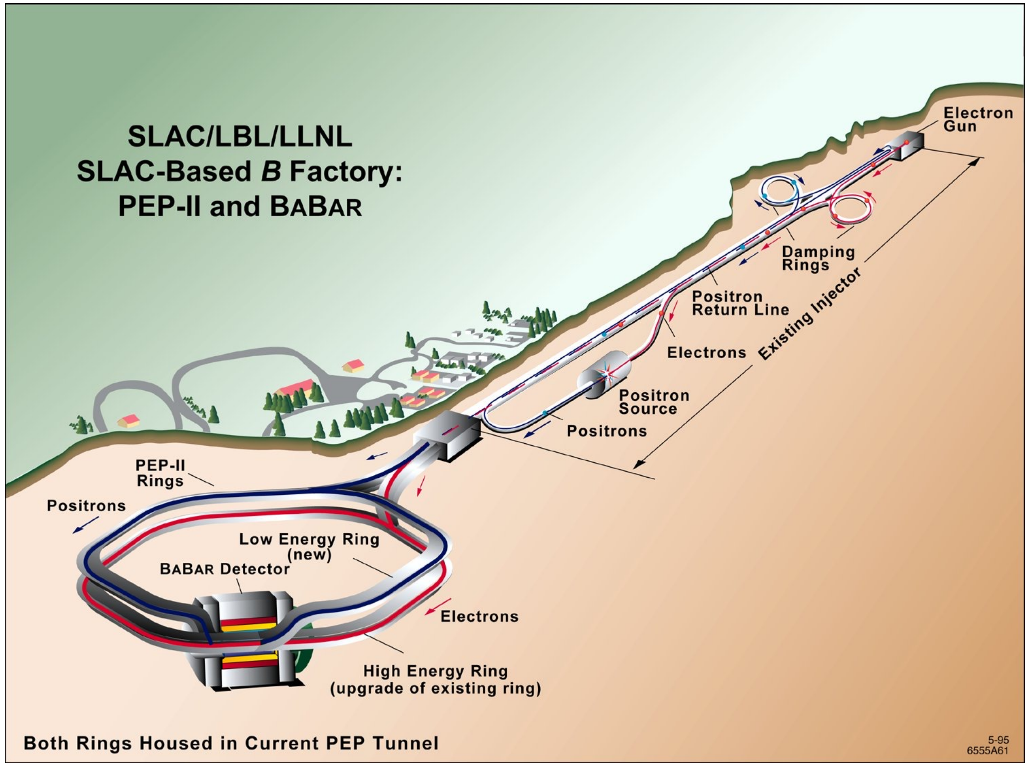

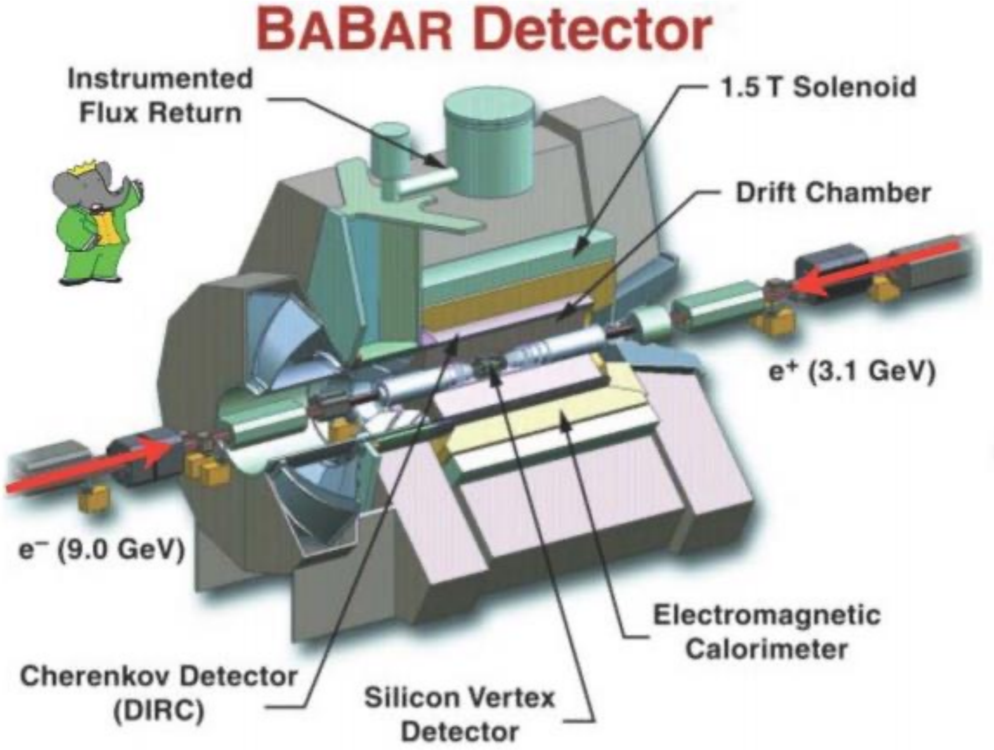

Advantages	**Known initial state, low backgrounds, good tagging efficiency (30%), good neutral detection, quantum correlated B production, almost hermetic detectors, good trigger efficiency for low multiplicity events**
Disadvantages	Production x-section ~1 nb, limited B_s production, no B_c, no high mass baryons, limited Υ(2,3,5S).

BaBar at SLAC PEP-II: 1999 – 2008 – Data Sample

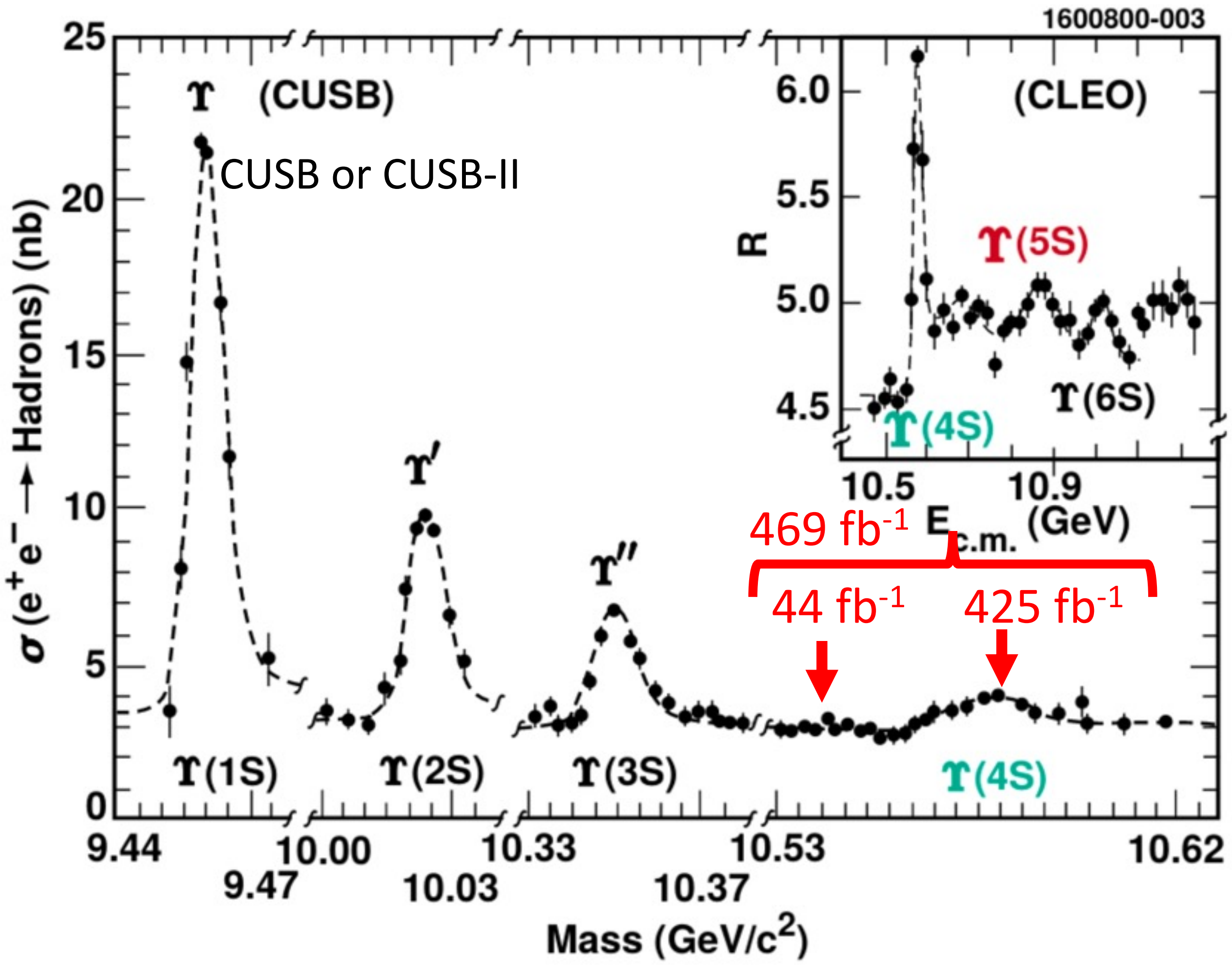

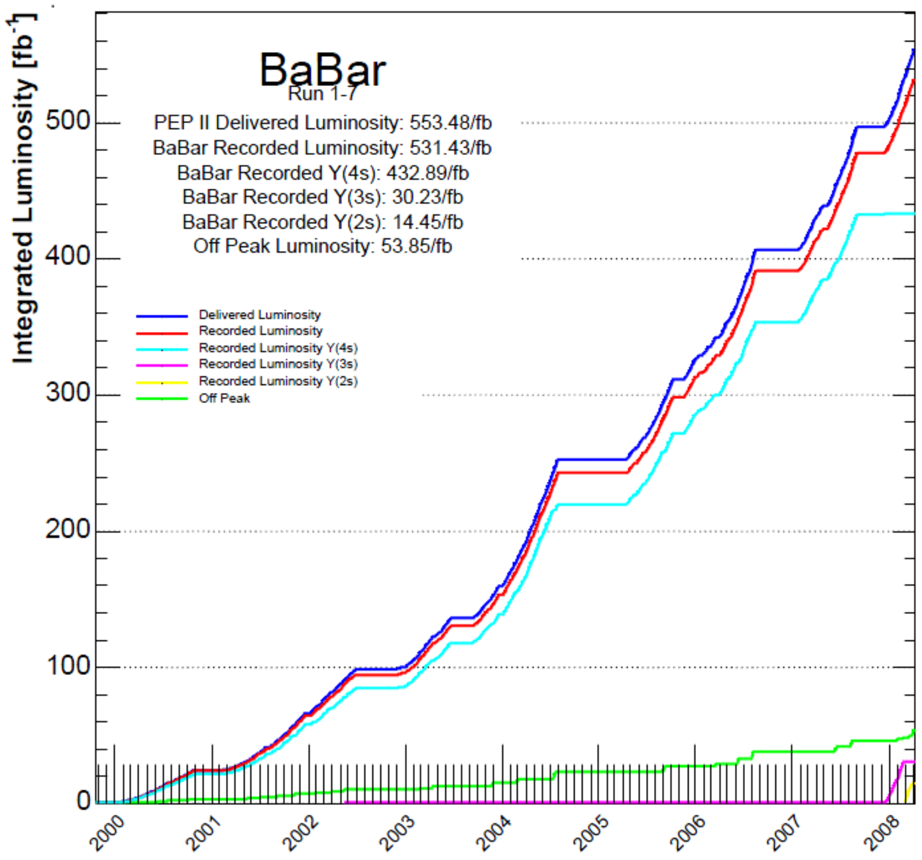

Science and Technology Facilities Council

BaBar and Initial State Radiation (ISR)

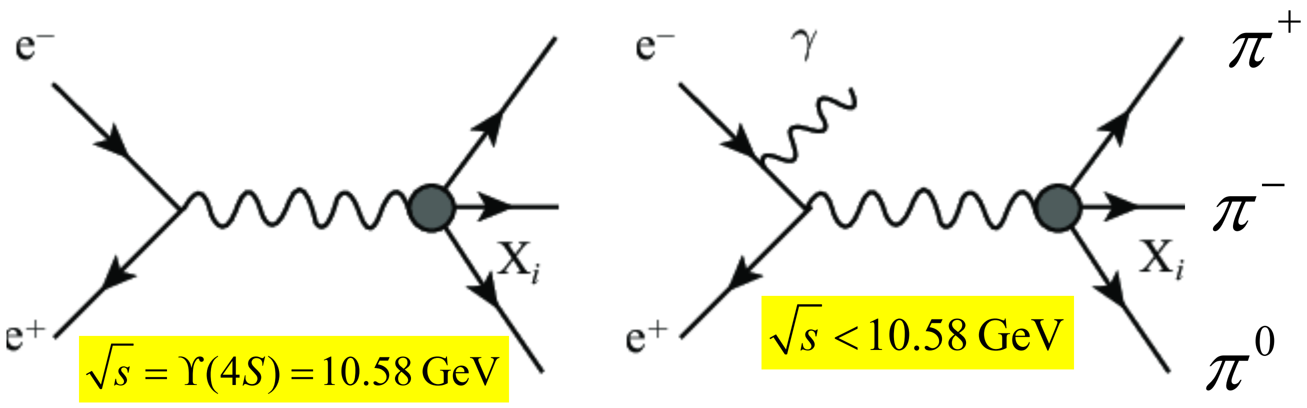

- Cross-sections can be measured down to threshold.
- Measure σ at all *s* simultaneously.
- About 10% of ISR γ's are produced in fiducial region of the BaBar detector.
- Tag event with presence of high energy ISR γ
- All hadrons in the detector.
- Fully reconstruct the final state.

$$\frac{d\sigma(s,x,\theta_\gamma)}{dx\, d\cos\theta_\gamma} = W(s,x,\theta_\gamma)\sigma_s(s(1-x))$$

$$W(s,x,\theta_\gamma) = \frac{\alpha}{2\pi}\left(\frac{2-2x+x^2}{\sin^2\theta_\gamma} - \frac{x^2}{2}\right)$$

$$x = 2E_\gamma / \sqrt{s}$$

$e^+e^- \longrightarrow \pi^+\pi^-\pi^0\gamma_{ISR}$ selection – General approach

- Two or more charged tracks + three or more γ's
  - One γ_{ISR} with high energy, other two with mass compatible with π^0
- Select events using a fit with kinematic constraints (cut on fit quality, χ^2)
- Reduce backgrounds through e.g.
  - Particle Identification (K/π), energy of π^0, mass of $\pi\pi$ and $\pi^\pm\gamma_{ISR}$ pairs, fit to alternative decay hypotheses (e.g. $e^+e^- \rightarrow \pi^+\pi^-\pi^0\pi^0\gamma$), …
- Remaining ISR and $q\bar{q}$ background subtraction:
  - $M_{3\pi} < 1.1$ GeV: use simulation, reweighted using data.
  - $M_{3\pi} > 1.1$ GeV: many ISR processes not simulated, so number of background events extrapolated using data from $20 < \chi^2 < 40$ region.

$e^+e^- \longrightarrow \pi^+\pi^-\pi^0\gamma_{ISR}$ event selection - details

- Two good oppositely charged tracks + 3 or more γ's
  - $0.10 < m(\pi^0) < 0.17$ GeV
  - Charged tracks not an electron and come from interaction region
- All hadrons + photons in the detector.
  - Charged tracks: $23^o < \theta < 140^o$ (in the lab); photons: $23^o < \theta < 137.5^o$ (overlaps with calorimeter)
- Tag event with presence of high energy ISR γ in centre of mass system
  - $E^*(\gamma_{ISR}) > 3$ GeV (prevents background from B decays)
- Fully reconstruct the final state.
- Select events using a kinematic fit (cut on fit quality, χ^2)
  - Constraints on energy and momentum conservation, π^0 mass
  - All π^0 in event are considered, take one with smallest χ^2
  - Require events to have $\chi^2 < 20$ (for $e^+e^- \rightarrow \pi^+\pi^-\pi^0$ cross-section measurement)
  - Use events with large χ^2 to rescale MC background simulation samples to predict backgrounds.

Background Suppression

- Main Backgrounds
  - ISR processes:
    - $e^+e^- \rightarrow \pi^+\pi^-\pi^0\pi^0\gamma$: kinematic fit to 4πγ hypothesis and reject if $\chi^2 < 30$
    - Two-body: $e^+e^- \rightarrow \pi^+\pi^-\gamma$, $\mu^+\mu^-\gamma$, + spurious γ : $E(\pi^0) > 0.4$ GeV/c and $M^2(\pi^+\pi^-) > 5$ GeV^2/c^4
    - Charged kaons: $e^+e^- \rightarrow K^+K^-\pi^0\gamma$: suppressed if identified as kaon by particle identification
    - + less important ISR backgrounds
  - Non-ISR processes: $e^+e^- \rightarrow q\bar{q}$ (q=u,d,s,c quark)
    - $e^+e^- \rightarrow \pi^+\pi^-\pi^0\pi^0$, $\tau^+\tau^-$: $M(\pi^\pm\gamma) > 1.5$ GeV/c^2
  - FSR processes:
    - PLACEHOLDER
- Remaining ISR and $q\bar{q}$ background subtraction:
  - $M_{3\pi} < 1.1$ GeV: use simulation, reweighted using data.
  - $M_{3\pi} > 1.1$ GeV: many ISR processes not simulated, so number of background events extrapolated using data from $20 < \chi^2 < 40$ region.
- Background suppression
  - $m(\pi^+\pi^-\pi^0) < 1.1$ GeV/c^2: Reduces background from 5% to 2% of data with 15% loss of signal
  - $1.05 < m(\pi^+\pi^-\pi^0) < 3.0$ GeV/c^2 : Reduces background by factor 2.6 with 17% loss of signal

Science and Technology Facilities Council

Backgrounds and Background Suppression

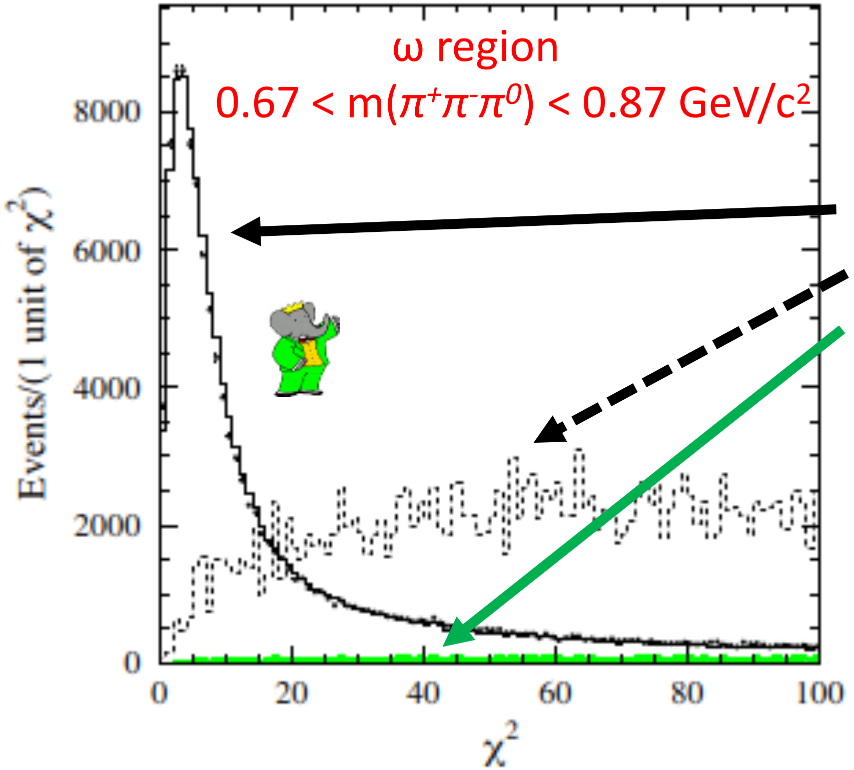

Minimal background

Data

Background (from MC) x 25

Background (from MC)

Background (from data)

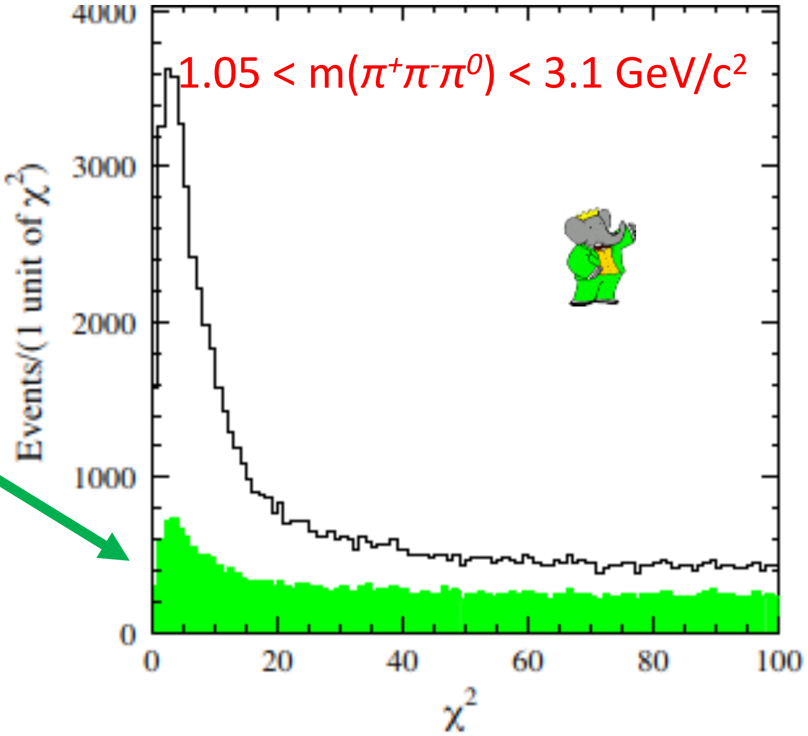

More background

Data after all criteria

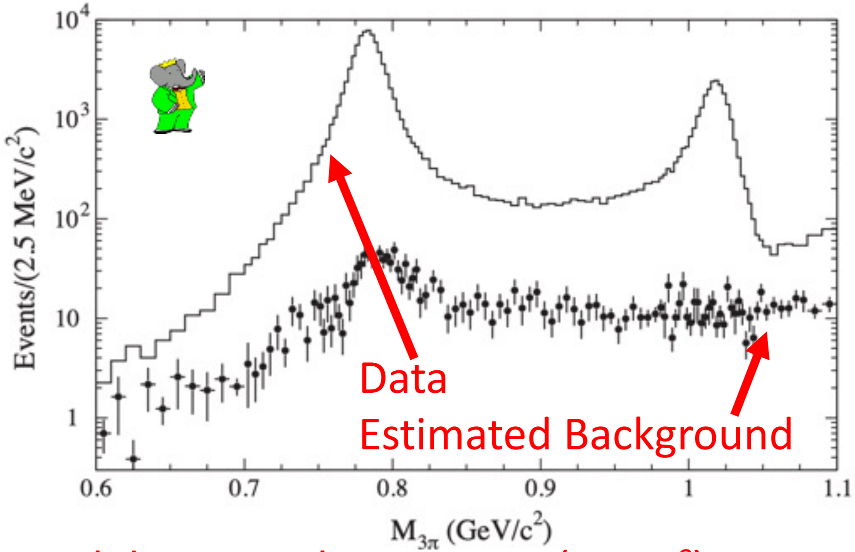

Final data sample in $0.6 < m(\pi^+\pi^-\pi^0) < 1.1$ GeV/c^2

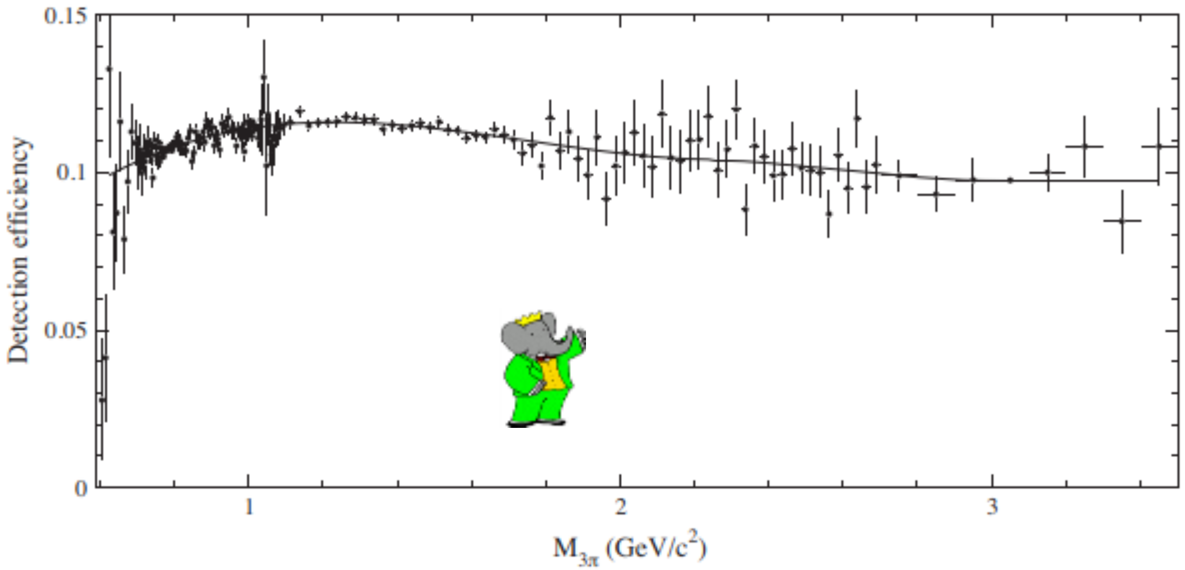

Detection efficiency obtained using simulated samples.

Statistical uncertainty: 0.1% near ω , 0.2% at ϕ, 1% near 2 GeV/c^2 and 2.2% at 2.5 GeV/c^2

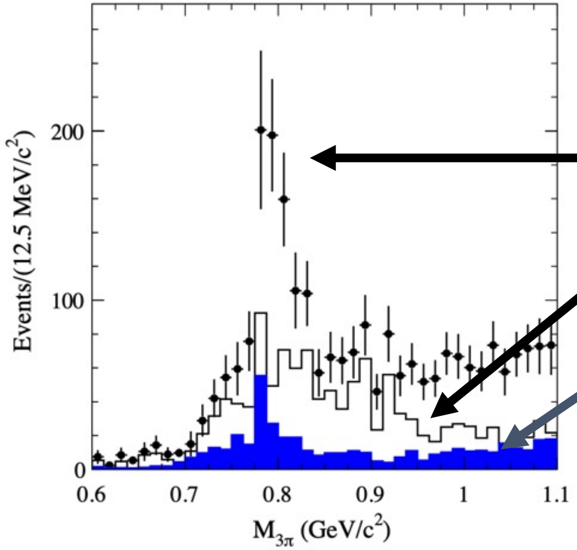

All backgrounds

All bckgs (less $e^+e^- \to \pi^+\pi^-\gamma$)

All bckgs (less $e^+e^- \to \pi^+\pi^-\pi^0\,\pi^0\gamma$, $e^+e^- \to \pi^+\pi^-\gamma$)

Unfolding Detector Resolution

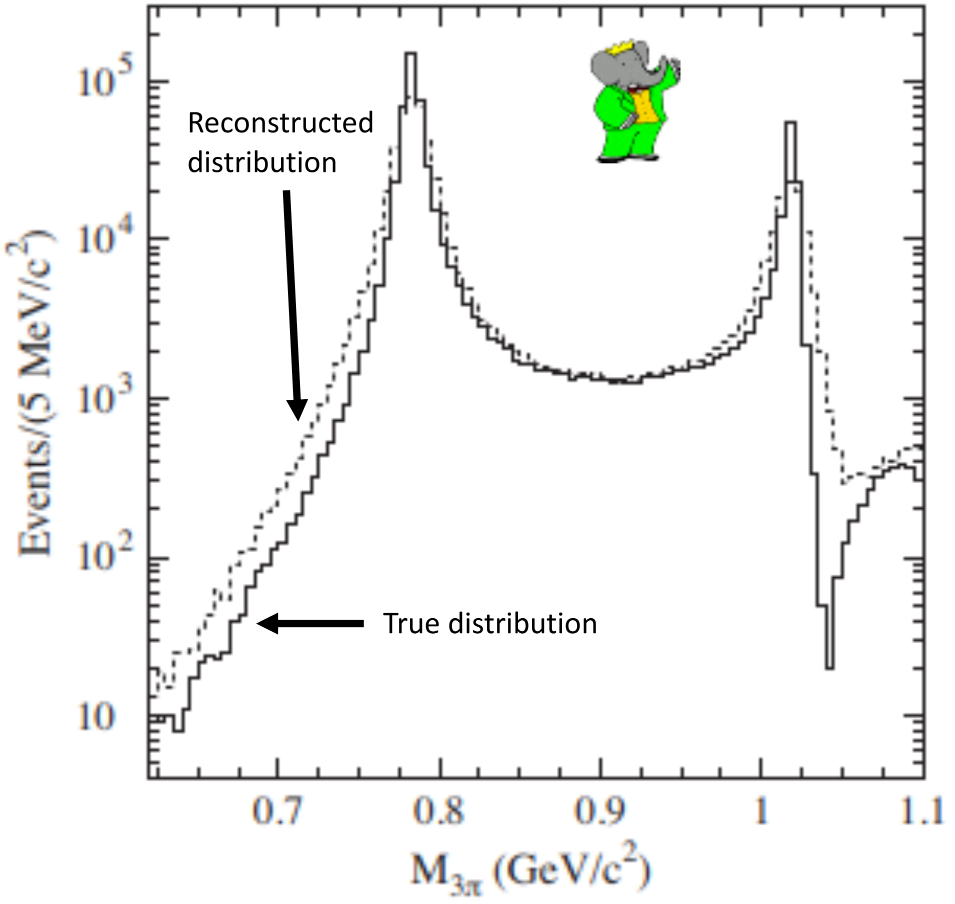

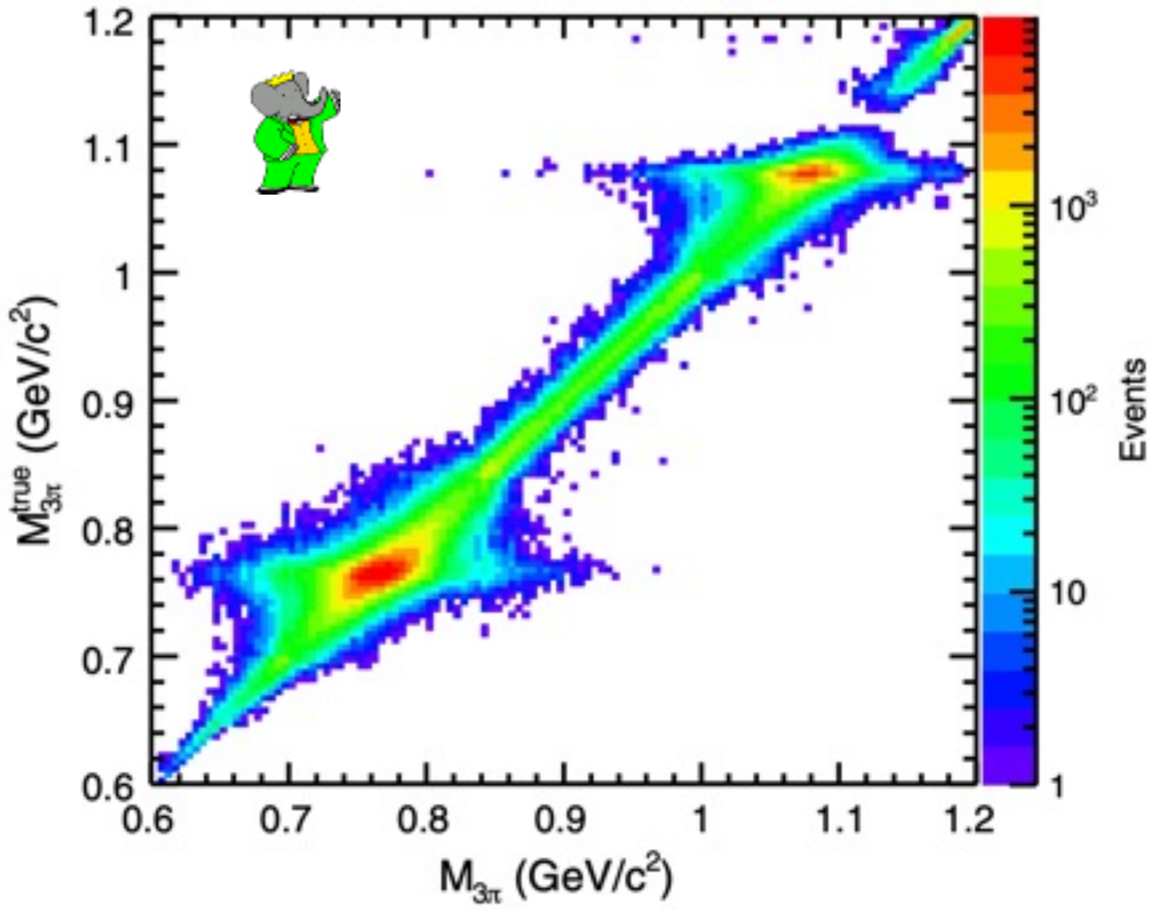

Science and Technology Facilities Council

$e^+e^- \longrightarrow \pi^+\pi^-\pi^0$ mass spectrum

Phys Rev D 104, 112003 (2021)

Fit with Vector Dominance Model (VDM) to $M_{3\pi}$ distribution with detector resolution effects unfolded:

Spectrum varies by 4 orders of magnitude and has two narrow peaks (ω,ϕ)

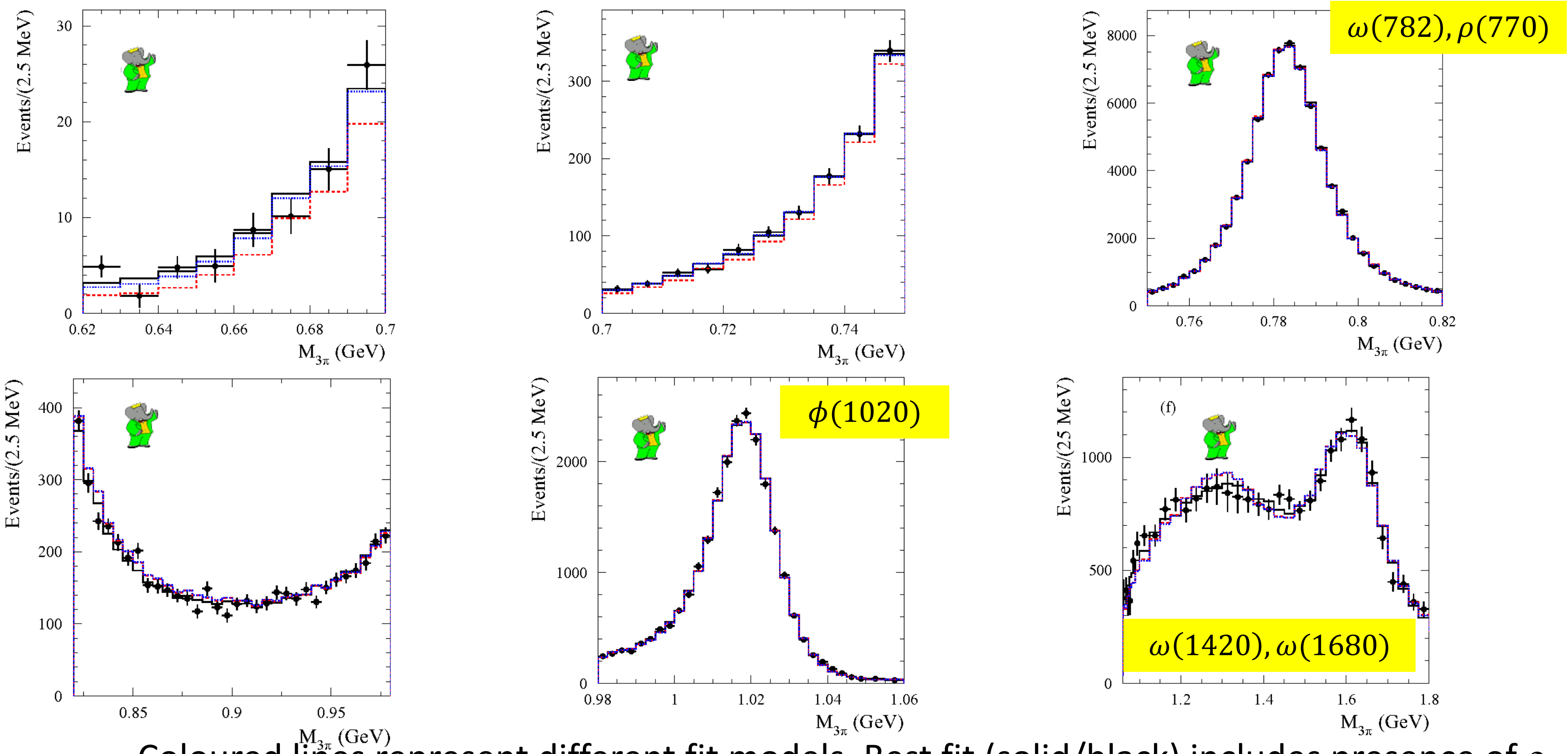

Coloured lines represent different fit models. Best fit (solid/black) includes presence of $\rho \rightarrow \pi\pi\pi$

Fit includes: $\omega(782)+\omega(1420)+\omega(1680)+\phi(1020)+\rho(770)\rightarrow 3\pi$

Science and Technology Facilities Council

$e^+e^- \longrightarrow \pi^+\pi^-\pi^0$ mass spectrum

Phys Rev D 104, 112003 (2021)

Fit includes: $\omega(782)+\omega(1420)+\omega(1680)+\phi(1020)+\rho(770)\rightarrow 3\pi$

Measurement	BABAR	Comparison
$\Gamma(\omega\to e^+e^-)B(\omega\to\pi^+\pi^-\pi^0)$	$(0.5698\pm0.0031\pm0.0082)$ keV	WA: (0.557 ± 0.011) keV
$\Gamma(\phi\to e^+e^-)B(\phi\to\pi^+\pi^-\pi^0)$	$(0.1841\pm0.0021\pm0.0080)$ keV	WA: (0.1925 ± 0.0043) keV
$B(\rho\to\pi^+\pi^-\pi^0)$	$(0.88\pm0.23\pm0.30)\times10^{-4}$	SND: $(1.01^{+0.54}_{-0.34}\pm0.34)\times10^{-4}$
$(\phi_\rho-\phi_\omega)^\circ$	$-(99\pm9\pm15)^\circ$	SND: $-(135^{+17}_{-13}\pm9)^\circ$

$e^+e^- \longrightarrow \pi^+\pi^-\pi^0$ cross-section: comparison with SND/CMD-2

Differences between experiments have been a source of systematic uncertainty on $(g\text{-}2)_\mu$ for some time

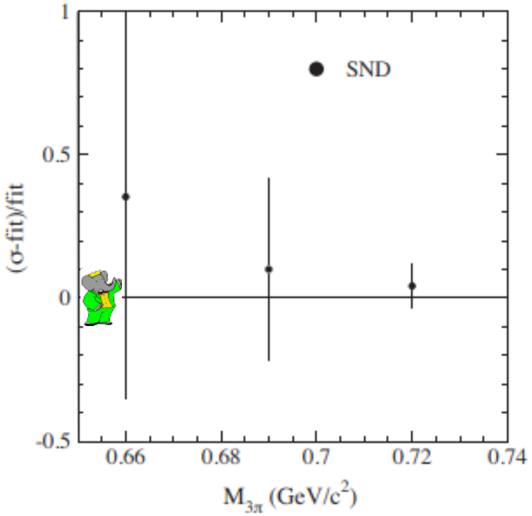

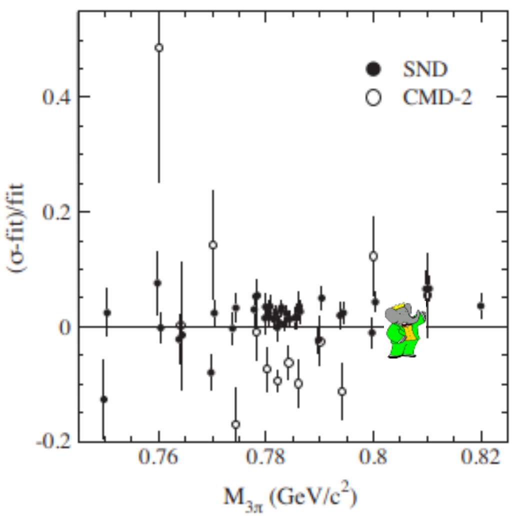

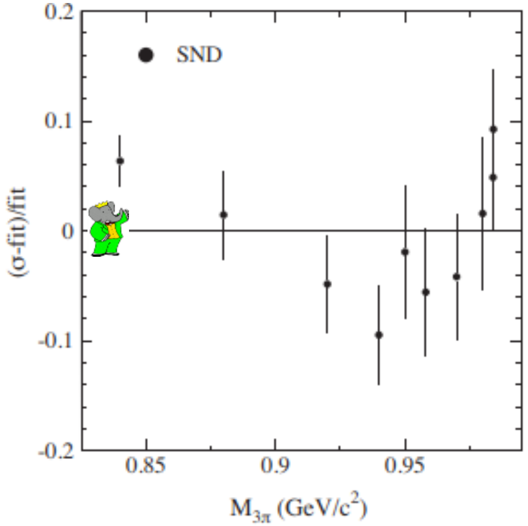

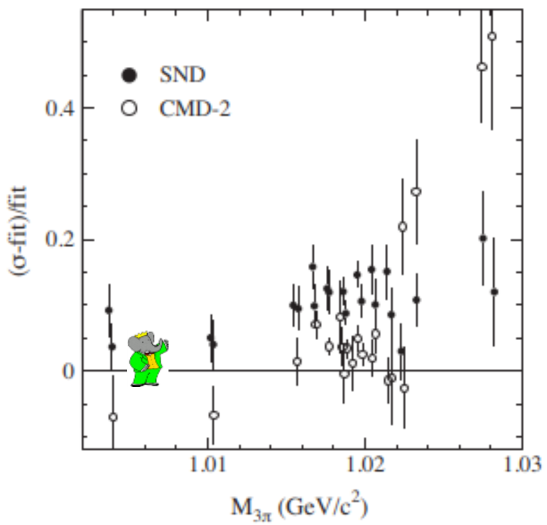

Good Agreement

Δ(SND-BaBar) = 2%
Δ(CMD-2-BaBar) = 7%

Good agreement

Δ(SND-BaBar) = 11%
Δ(CMD-2-BaBar) = 3%

SND results: [3], [4], [7] ; CMD-2 results [5], [6]

$e^+e^- \longrightarrow \pi^+\pi^-\pi^0$ cross-section: comparison with SND

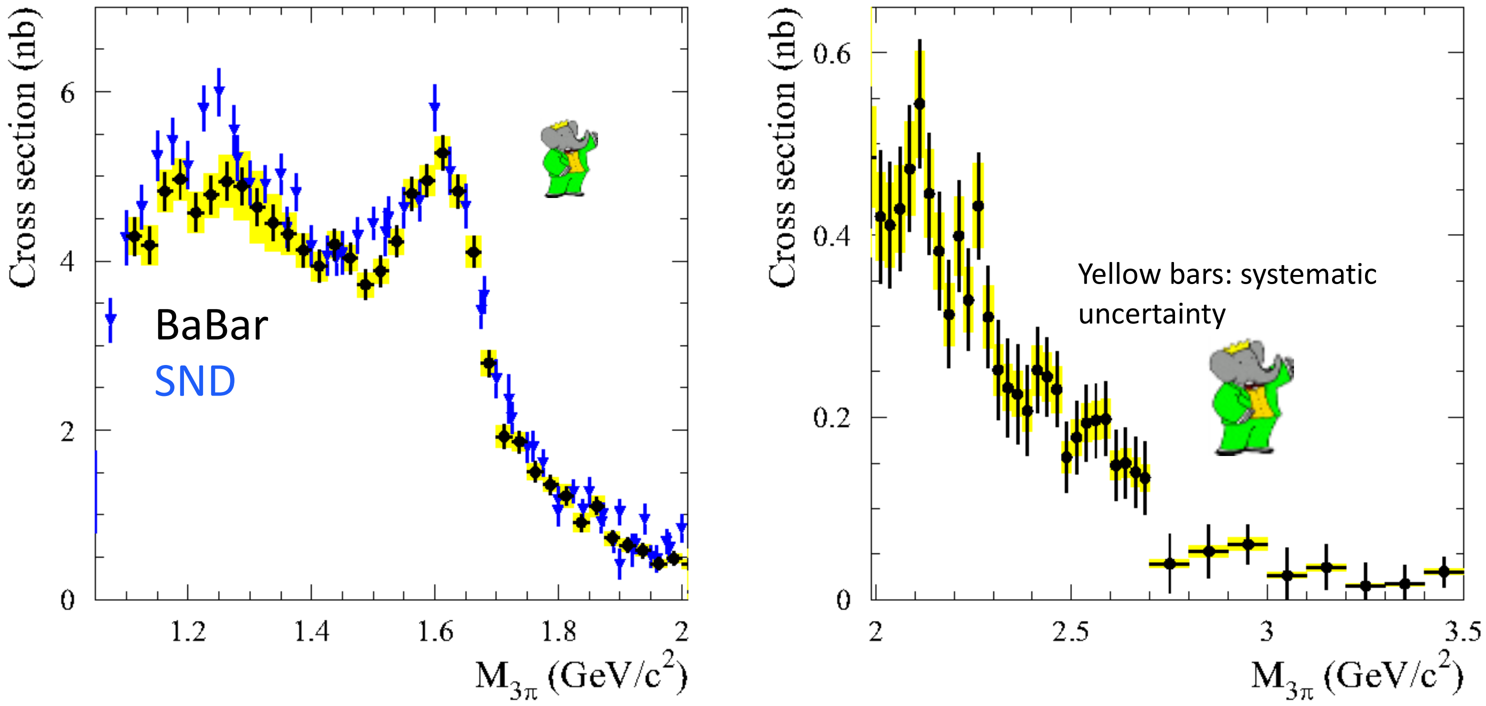

Generally good agreement but differences between SND and BaBar near 1.25 and 1.5 GeV

SND results: [3], [4], [7] ; CMD-2 results [5], [6]

$e^+e^- \longrightarrow \pi^+\pi^-\pi^0$ contribution to $(g\text{-}2)_\mu$

$M_{3\pi}$ [GeV/c^2]	$a_\mu^{3\pi}$ [10^{-10}]	Reference
$0.62 - 1.10$	$42.91 \pm 0.14 \pm 0.55 \pm 0.09$	BABAR Phys. Rev. D104, 112003 (2021)
$1.10 - 2.00$	$2.95 \pm 0.03 \pm 0.16$	BABAR Phys. Rev. D104, 112003 (2021)
< 2.00	$45.86 \pm 0.14 \pm 0.58$	BABAR Phys. Rev. D104, 112003 (2021)
< 1.80	$42.61 \pm 0.40 \pm 1.40$	Eur. Phys. J. C80, 241 (2020)
< 1.97	46.74 ± 0.94	Phys. Rev. D101, 014029 (2020)
< 2.00	44.32 ± 1.48	Springer Tracts Mod. Phys. 274, 1 (2017)

Differences in 3π mass scales between experiments;
Estimated from differences in BaBar/SND/CMD-2 data

Effect	Uncertainty (%)
Luminosity	0.4
Radiative correction	0.5
Detection efficiency	1.1
MC statistics	0.15
Background subtraction	0.073
Gaussian smearing	0.0007
Lorentzian smearing	0.003
Unfolding procedure	0.045
Total	1.3

Quick summary of other recent BaBar ISR results

- Measurements of $e^+e^- \longrightarrow \pi^+\pi^-4\pi^0$ cross-section
  - Phys Rev D 104, 112004 (2021)
- Measurements of $e^+e^- \longrightarrow 2(\pi^+\pi^-)3\pi^0$ cross-section
  - Phys Rev D 103, 092001 (2021)
- Preliminary measurements of $e^+e^- \longrightarrow KK\pi\pi\pi$ cross-sections
  - arXiv:2207.10340 (2022)
- These processes contribute $\lesssim$ 0.5% to $a_\mu^{Had,LO}$ and $\lesssim$ 1.5% to the uncertainty

$e^+e^- \longrightarrow \pi^+\pi^-4\pi^0$

Phys Rev D 104, 112004 (2021)

- Similar selection technique to $e^+e^- \longrightarrow \pi^+\pi^-\pi^0$
- Same integrated luminosity (469 fb^{-1})
- Many branching fractions and cross-sections measured for the first time.

Statistical uncertainty 12%-15%

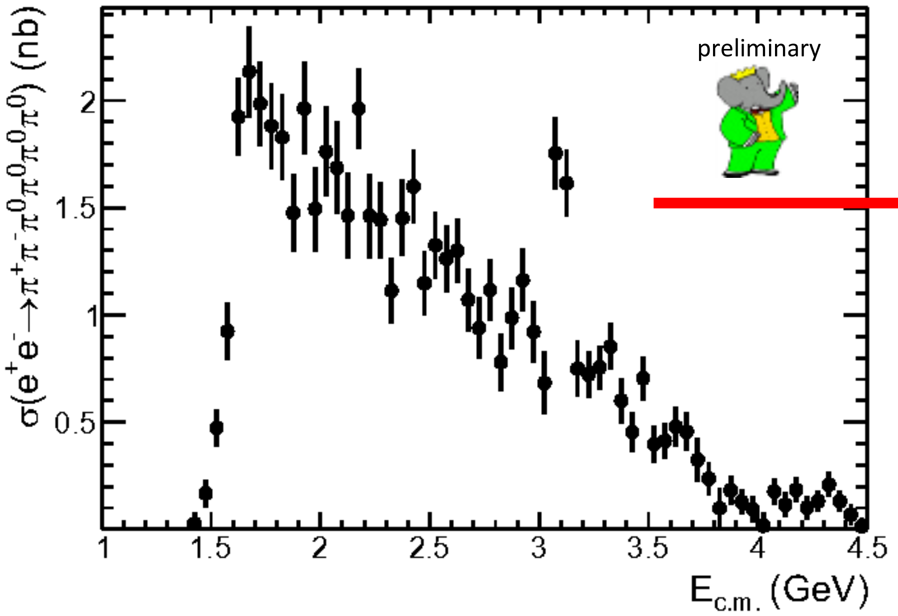

TABLE I: Summary of the $e^+e^- \to \pi^+\pi^-\pi^0\pi^0\pi^0\pi^0$ cross section measurement. The uncertainties are statistical only.

$E_{c.m.}$ (GeV)	σ (nb)	$E_{c.m.}$ (GeV)	σ (nb)	$E_{c.m.}$ (GeV)	σ (nb)	$E_{c.m.}$ (GeV)	σ (nb)	$E_{c.m.}$ (GeV)	σ (nb)
1.425	0.03 ± 0.05	2.075	1.69 ± 0.21	2.725	0.94 ± 0.14	3.375	0.60 ± 0.10	4.025	0.02 ± 0.06
1.475	0.17 ± 0.06	2.125	1.46 ± 0.20	2.775	1.12 ± 0.14	3.425	0.45 ± 0.09	4.075	0.18 ± 0.06
1.525	0.47 ± 0.08	2.175	1.96 ± 0.19	2.825	0.78 ± 0.13	3.475	0.71 ± 0.10	4.125	0.11 ± 0.06
1.575	0.92 ± 0.13	2.225	1.46 ± 0.19	2.875	0.99 ± 0.14	3.525	0.40 ± 0.08	4.175	0.18 ± 0.06
1.625	1.92 ± 0.18	2.275	1.44 ± 0.18	2.925	1.16 ± 0.14	3.575	0.41 ± 0.08	4.225	0.10 ± 0.05
1.675	2.13 ± 0.21	2.325	1.11 ± 0.15	2.975	0.92 ± 0.14	3.625	0.48 ± 0.09	4.275	0.13 ± 0.05
1.725	1.99 ± 0.20	2.375	1.45 ± 0.18	3.025	0.68 ± 0.15	3.675	0.46 ± 0.09	4.325	0.21 ± 0.06
1.775	1.88 ± 0.20	2.425	1.60 ± 0.17	3.075	1.75 ± 0.17	3.725	0.32 ± 0.10	4.375	0.13 ± 0.05
1.825	1.83 ± 0.20	2.475	1.15 ± 0.15	3.125	1.61 ± 0.16	3.775	0.24 ± 0.08	4.425	0.07 ± 0.05
1.875	1.48 ± 0.18	2.525	1.33 ± 0.16	3.175	0.75 ± 0.13	3.825	0.10 ± 0.09	4.475	0.01 ± 0.04
1.925	1.96 ± 0.21	2.575	1.26 ± 0.16	3.225	0.72 ± 0.10	3.875	0.18 ± 0.07		
1.975	1.49 ± 0.20	2.625	1.30 ± 0.15	3.275	0.75 ± 0.10	3.925	0.13 ± 0.06		
2.025	1.76 ± 0.21	2.675	1.07 ± 0.14	3.325	0.85 ± 0.11	3.975	0.10 ± 0.06		

- Also includes cross-sections for $e^+e^- \longrightarrow \omega 3\pi^0$, $\eta\pi^+\pi^-\pi^0$ and $\omega\eta$

$e^+e^- \longrightarrow 2(\pi^+\pi^-)3\pi^0$ and $e^+e^- \longrightarrow 2(\pi^+\pi^-)2\pi^0\eta$ PRD 103, 092001 (2021)

- Similar selection technique again.
- Same integrated luminosity (469 fb^{-1}).
- Many branching fractions and cross-sections measured for the first time.

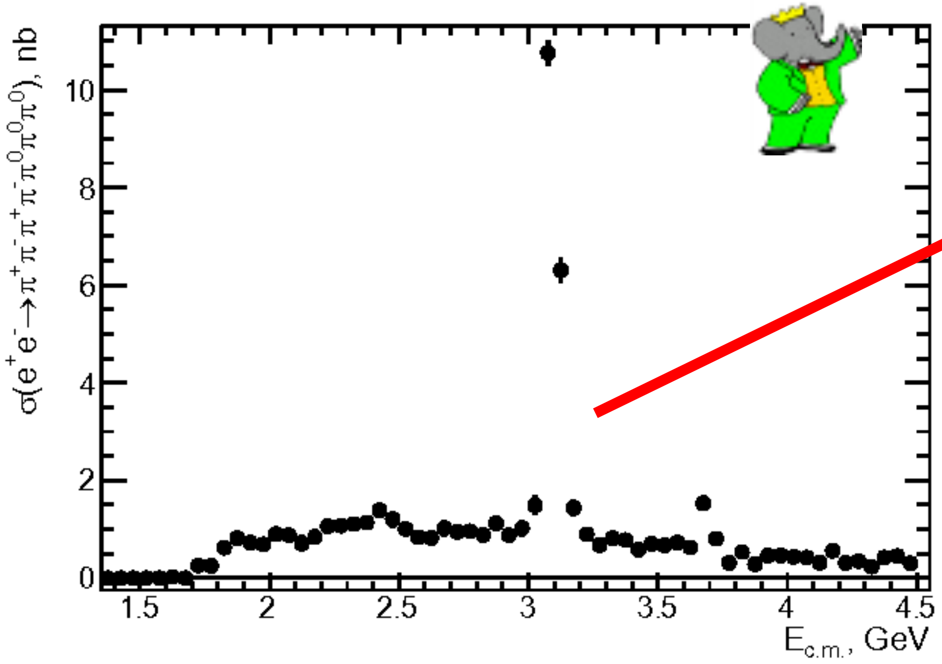

TABLE I. Summary of the $e^+e^- \to 2(\pi^+\pi^-)3\pi^0$ cross section measurement. The uncertainties are statistical only.

$E_{c.m.}$ (GeV)	σ (nb)	$E_{c.m.}$ (GeV)	σ (nb)	$E_{c.m.}$ (GeV)	σ (nb)	$E_{c.m.}$ (GeV)	σ (nb)	$E_{c.m.}$ (GeV)	σ (nb)
1.575	0.00 ± 0.01	2.175	0.84 ± 0.15	2.775	0.96 ± 0.14	3.375	0.78 ± 0.12	3.975	0.46 ± 0.09
1.625	0.02 ± 0.01	2.225	1.06 ± 0.11	2.825	0.88 ± 0.13	3.425	0.59 ± 0.09	4.025	0.44 ± 0.09
1.675	0.00 ± 0.02	2.275	1.07 ± 0.14	2.875	1.12 ± 0.13	3.475	0.70 ± 0.11	4.075	0.42 ± 0.09
1.725	0.26 ± 0.06	2.325	1.11 ± 0.12	2.925	0.88 ± 0.13	3.525	0.67 ± 0.10	4.125	0.32 ± 0.07
1.775	0.25 ± 0.07	2.375	1.14 ± 0.14	2.975	1.02 ± 0.17	3.575	0.73 ± 0.12	4.175	0.56 ± 0.08
1.825	0.62 ± 0.09	2.425	1.39 ± 0.16	3.025	1.49 ± 0.20	3.625	0.63 ± 0.11	4.225	0.31 ± 0.08
1.875	0.82 ± 0.14	2.475	1.21 ± 0.16	3.075	10.76 ± 0.26	3.675	1.53 ± 0.15	4.275	0.35 ± 0.06
1.925	0.73 ± 0.09	2.525	1.01 ± 0.16	3.125	6.30 ± 0.26	3.725	0.81 ± 0.13	4.325	0.23 ± 0.07
1.975	0.69 ± 0.10	2.575	0.84 ± 0.14	3.175	1.44 ± 0.15	3.775	0.31 ± 0.11	4.375	0.42 ± 0.06
2.025	0.90 ± 0.15	2.625	0.82 ± 0.11	3.225	0.90 ± 0.11	3.825	0.53 ± 0.10	4.425	0.45 ± 0.07
2.075	0.88 ± 0.14	2.675	1.02 ± 0.15	3.275	0.67 ± 0.12	3.875	0.29 ± 0.09	4.475	0.30 ± 0.07
2.125	0.70 ± 0.16	2.725	0.95 ± 0.15	3.325	0.82 ± 0.12	3.925	0.46 ± 0.09		

- Paper also includes cross-sections for *$e^+e^- \longrightarrow \omega\, \pi^+\pi^-\pi^0\pi^0$, $\eta\pi^+\pi^-\pi^0\pi^0$ and $\eta 2(\pi^+\pi^-)$*

$e^+e^- \to K^+K^-3\pi^0$, $K^0_sK^\pm\pi^{-/+}\pi^0\pi^0$, $K^0_sK^\pm\pi^{-/+}\pi^+\pi^-$ arXiv:2207.10340 (2022)

- Similar selection technique again. Same integrated luminosity (469 fb^{-1}).
- Only the $e^+e^- \to K^+K^-3\pi^0$ reaction has been previously studied.
  - Simulated with $e^+e^- \to \varphi(1020)\eta$
  - For two other modes use phase space
- For modes with neutral pions:
  - Require all but one π^0 to have $|m(\gamma\gamma) - m(\pi^0)| < 35$ MeV/c^2.
  - Try all combinations of $\gamma\gamma$ pairs, take the decay candidate with the best χ^2 fit.
  - Fit the m($\gamma\gamma$) distribution of the remaining $\gamma\gamma$ pair in bins of $m(K^+K^-2\pi^0\gamma\gamma)$ or $m(K^0_sK^\pm\pi^{-/+}\pi^0\gamma\gamma)$.
- For $K^0_sK^\pm\pi^{-/+}\pi^+\pi^-$, use fit to χ^2 distribution

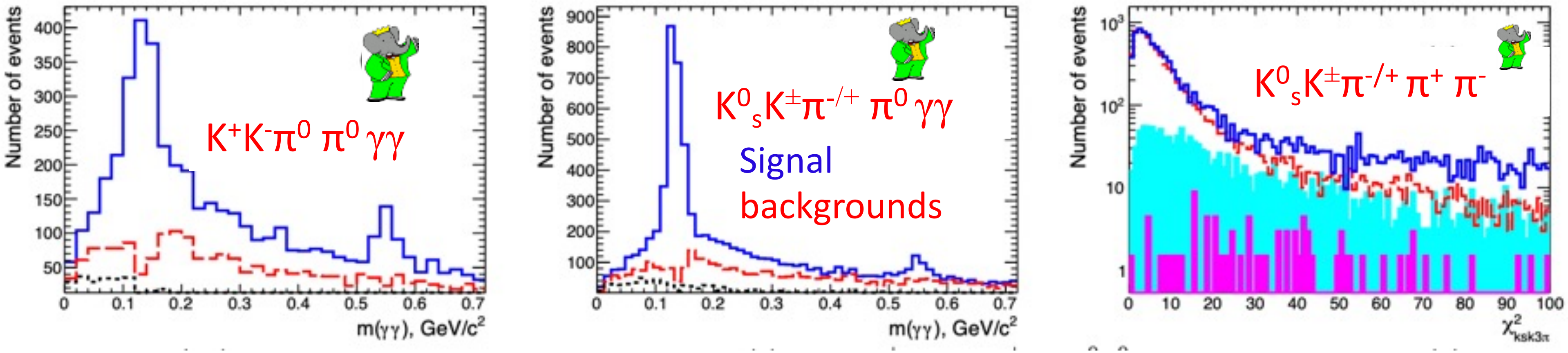

Distributions (preliminary)

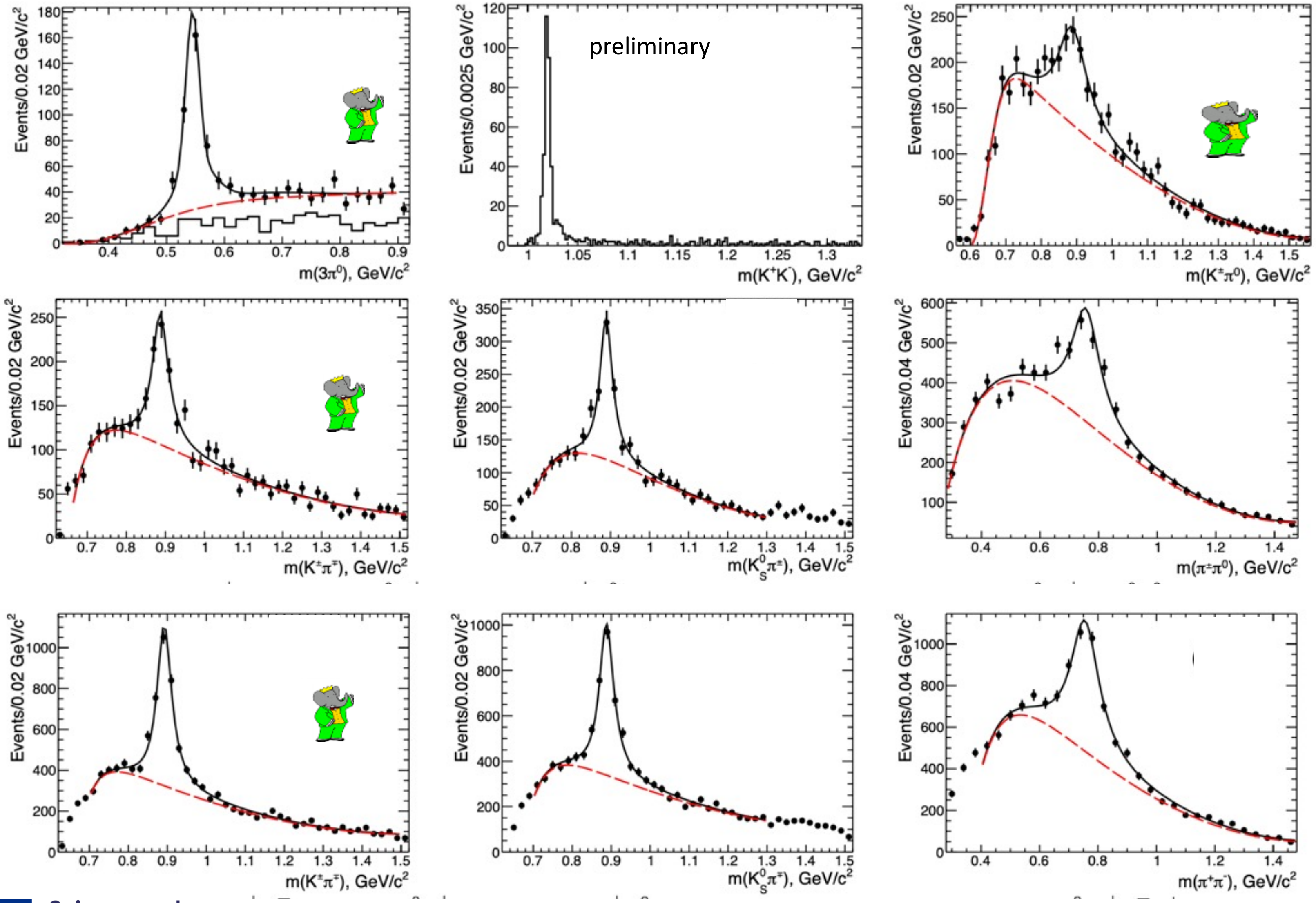

$e^+e^- \longrightarrow K^+K^-3\pi^0$

$e^+e^- \longrightarrow K^0_sK^\pm\pi^\mp\pi^0\,\pi^0$

$e^+e^- \longrightarrow K^0_sK^\pm\pi^\mp\pi^+\,\pi^-$

Results

TABLE II: Summary of the J/ψ and $\psi(2S)$ branching fractions. Each value is quoted with its statistical and systematic uncertainties.

Measured Quantity	Measured Value (eV)	J/ψ or $\psi(2S)$ Branching Fraction (10^{-3}) Derived, this work	PDG [30]
$\Gamma_{ee}^{J/\psi}\cdot B_{J/\psi\to K^+K^-\pi^0\pi^0\pi^0}$	8.9 ±1.3 ±0.9	1.6 ±0.2 ±0.2	no entry
$\Gamma_{ee}^{J/\psi}\cdot B_{J/\psi\to\eta K^+K^-}\cdot B_{\eta\to\pi^0\pi^0\pi^0}$	1.55±0.51±0.16	0.85±0.28±0.09	no entry
$\Gamma_{ee}^{J/\psi}\cdot B_{J/\psi\to\phi\eta}\cdot B_{\phi\to K^+K^-}\cdot B_{\eta\to\pi^0\pi^0\pi^0}$	0.64±0.26±0.06	0.72±0.29±0.07	0.74±0.08
$\Gamma_{ee}^{J/\psi}\cdot B_{J/\psi\to K^{*+}K^{*-}\pi^0}\cdot B_{K^{*+}\to K^+\pi^0}\cdot B_{K^{*-}\to K^-\pi^0}$	6.9 ±1.2 ±0.7	5.0 ±0.9 ±0.5	no entry
$\Gamma_{ee}^{\psi(2S)}\cdot B_{\psi(2S)\to K^+K^-\pi^0\pi^0\pi^0}$	1.54±0.63±0.15	0.66±0.27±0.07	no entry
$\Gamma_{ee}^{\psi(2S)}\cdot B_{\psi(2S)\to J/\psi\pi^0\pi^0}\cdot B_{J/\psi\to K^+K^-\pi^0}$	1.31±0.35±0.13	3.1 ±0.8 ±0.3	2.88±0.13
$\Gamma_{ee}^{\psi(2S)}\cdot B_{\psi(2S)\to\eta K^+K^-}\cdot B_{\eta\to\pi^0\pi^0\pi^0}$	<0. 2 at 90% C.L.	<0. 25 at 90% C.L.	no entry
$\Gamma_{ee}^{\psi(2S)}\cdot B_{\psi(2S)\to K^{*+}K^{*-}\pi^0}\cdot B_{K^{*+}\to K^+\pi^0}\cdot B_{K^{*-}\to K^-\pi^0}$	0.94±0.45±0.10	1.6 ±0.8 ±0.2	no entry
$\Gamma_{ee}^{J/\psi}\cdot B_{J/\psi\to K^0_SK^\pm\pi^\mp\pi^0\pi^0}$	29.3 ±2.6 ±2.9	5.3 ±0.5 ±0.5	no entry
$\Gamma_{ee}^{J/\psi}\cdot B_{J/\psi\to K^{*\pm}K^\mp\pi^0\pi^0}\cdot B_{K^{*\pm}\to K^0\pi^\pm}\cdot B_{K^0\to K^0_S}$	2.89±0.52±0.28	2.0 ±0.4 ±0.2	no entry
$\Gamma_{ee}^{J/\psi}\cdot B_{J/\psi\to K^0K^{*0}\pi^0\pi^0}\cdot B_{K^{*0}\to K^\pm\pi^\mp}\cdot B_{K^0\to K^0_S}$	3.73±0.53±0.37	2.7 ±0.4 ±0.3	no entry
$\Gamma_{ee}^{J/\psi}\cdot B_{J/\psi\to K^0_SK^\pm\rho^\mp\pi^0}$	16.0 ±4.1 ±1.6	2.9 ±0.7 ±0.3	no entry
$\Gamma_{ee}^{\psi(2S)}\cdot B_{\psi(2S)\to K^0_SK^\pm\pi^\mp\pi^0\pi^0}$	4.0 ±1.4 ±0.4	1.7 ±0.6 ±0.2	no entry
$\Gamma_{ee}^{\psi(2S)}\cdot B_{\psi(2S)\to J/\psi\pi^0\pi^0}\cdot B_{J/\psi\to K^0_SK^\pm\pi^\mp}$	2.36±0.59±0.24	5.5 ±1.4 ±0.6	5.6 ±0.5
$\Gamma_{ee}^{\psi(2S)}\cdot B_{\psi(2S)\to K^{*\pm}K^\mp\pi^0\pi^0}\cdot B_{K^{*\pm}\to K^0\pi^\pm}\cdot B_{K^0\to K^0_S}$	0.54±0.22±0.05	0.92±0.37±0.09	no entry
$\Gamma_{ee}^{\psi(2S)}\cdot B_{\psi(2S)\to K^0K^{*0}\pi^0\pi^0}\cdot B_{K^{*0}\to K^\pm\pi^\mp}\cdot B_{K^0\to K^0_S}$	0.47±0.19±0.05	0.81±0.32±0.08	no entry
$\Gamma_{ee}^{\psi(2S)}\cdot B_{\psi(2S)\to K^0_SK^\pm\rho^\mp\pi^0}$	<1. 6 at 90% C.L.	<0. 6 at 90% C.L.	no entry
$\Gamma_{ee}^{J/\psi}\cdot B_{J/\psi\to K^0_SK^\pm\pi^\mp\pi^+\pi^-}$	34.6 ±1.4 ±1.8	6.2 ±0.2 ±0.4	no entry
$\Gamma_{ee}^{J/\psi}\cdot B_{J/\psi\to K^{*\pm}K^{*0}\pi^\mp}\cdot B_{K^{*\pm}\to K^0\pi^\pm}\cdot B_{K^{*0}\to K^\pm\pi^\mp}\cdot B_{K^0\to K^0_S}$	5.9 ±1.0 ±0.6	8.5 ±1.5 ±0.9	no entry
$\Gamma_{ee}^{J/\psi}\cdot B_{J/\psi\to K^{*\pm}K^\mp\pi^+\pi^-}\cdot B_{K^{*\pm}\to K^0\pi^\pm}\cdot B_{K^0\to K^0_S}$	6.2 ±2.1 ±0.6	4.4 ±1.5 ±0.4	no entry
$\Gamma_{ee}^{J/\psi}\cdot B_{J/\psi\to K^0K^{*0}\pi^+\pi^-}\cdot B_{K^{*0}\to K^\pm\pi^\mp}\cdot B_{K^0\to K^0_S}$	6.3 ±2.1 ±0.6	4.5 ±1.5 ±0.5	no entry
$\Gamma_{ee}^{J/\psi}\cdot B_{J/\psi\to K^0_SK^\pm\pi^\mp\rho^0}$	17.3 ±2.1 ±1.7	3.1 ±0.4 ±0.3	no entry
$\Gamma_{ee}^{\psi(2S)}\cdot B_{\psi(2S)\to K^0_SK^\pm\pi^\mp\pi^+\pi^-}$	5.1 ±0.7 ±0.4	2.2 ±0.3 ±0.2	no entry
$\Gamma_{ee}^{\psi(2S)}\cdot B_{\psi(2S)\to J/\psi\pi^+\pi^-}\cdot B_{J/\psi\to K^0_SK^\pm\pi^\mp}$	4.14±0.55±0.29	5.1 ±0.7 ±0.1	5.6 ±0.5
$\Gamma_{ee}^{\psi(2S)}\cdot B_{\psi(2S)\to K^0_SK^\pm\pi^\mp\rho^0}$	<1. 6 at 90% C.L.	<0. 6 at 90% C.L.	no entry

$e^+e^- \longrightarrow K^+K^-3\pi^0$, $K^0{}_sK^\pm\pi^{-/+}\pi^0\pi^0$, $K^0{}_sK^\pm\pi^{-/+}\pi^+\pi^-$ cross sections measured with ± 10% accuracy.

New information on hadron spectroscopy.

Many subdecays measured for the first time.

Conclusion

- We present a number of recent measurements of the process $e^+e^- \rightarrow hadrons + \gamma_{ISR}$
- Cross-sections can be measured from threshold up to ~4.5 GeV
- Cross-sections for $e^+e^- \rightarrow 2(\pi^+\pi^-)3\pi^0$, $2(\pi^+\pi^-)2\pi^0\eta$, $\pi^+\pi^-4\pi^0$, and $\pi^+\pi^-3\pi^0\eta$ have been measured for the first time, using the ISR method with 469 fb^{-1} of data collected by BaBar at PEP-II at SLAC [Phys Rev D 104, 112004 (2021), PRD 103, 092001 (2021)]
- Many intermediate branching fractions have been measured for the first time for $e^+e^- \rightarrow K^+K^-3\pi^0$, $K^0_sK^\pm\pi^{-/+}\pi^0\pi^0$, and $K^0_sK^\pm\pi^{-/+}\pi^+\pi^-$ [arXiv:2207.10340 (2022)]
- The cross-section for $e^+e^- \rightarrow \pi^+\pi^-\pi^0$ has been measured in the centre of mass range 0.62 – 3.5 GeV. [Phys Rev D 104, 112003 (2021)]
- The leading order hadronic contribution of $e^+e^- \rightarrow \pi^+\pi^-\pi^0$ to the muon anomalous magnetic moment has been calculated as $(45.86 \pm 0.14 \pm 0.58) \times 10^{-10}$ for $M_{3\pi} < 2.0$ GeV:
    - The contribution is in agreement with existing calculations but a factor of two more precise.